



Article

Spontaneous Imbibition Oil Recovery by Natural Surfactant/Nanofluid: An Experimental and Theoretical Study

Reza Khoramian ¹, Riyaz Kharrat ² , Peyman Pourafshary ^{1,*} , Saeed Golshokoh ³ and Fatemeh Hashemi ⁴¹ School of Mining and Geosciences, Nazarbayev University, Astana 010000, Kazakhstan² Department Petroleum Engineering, Montanuniversität, 8700 Leoben, Austria³ Faculty of Petroleum and Natural Gas Engineering, Sahand University of Technology, Tabriz 513351996, Iran⁴ Faculty of Chemistry, Shiraz University, Shiraz 7155713876, Iran

* Correspondence: peyman.pourafshary@nu.edu.kz

Abstract: Organic surfactants have been utilized with different nanoparticles in enhanced oil recovery (EOR) operations due to the synergic mechanisms of nanofluid stabilization, wettability alteration, and oil-water interfacial tension reduction. However, investment and environmental issues are the main concerns to make the operation more practical. The present study introduces a natural and cost-effective surfactant named Azarboo for modifying the surface traits of silica nanoparticles for more efficient EOR. Surface-modified nanoparticles were synthesized by conjugating negatively charged Azarboo surfactant on positively charged amino-treated silica nanoparticles. The effect of the hybrid application of the natural surfactant and amine-modified silica nanoparticles was investigated by analysis of wettability alteration. Amine-surfactant-functionalized silica nanoparticles were found to be more effective than typical nanoparticles. Amott cell experiments showed maximum imbibition oil recovery after nine days of treatment with amine-surfactant-modified nanoparticles and fifteen days of treatment with amine-modified nanoparticles. This finding confirmed the superior potential of amine-surfactant-modified silica nanoparticles compared to amine-modified silica nanoparticles. Modeling showed that amine surfactant-treated SiO₂ could change wettability from strongly oil-wet to almost strongly water-wet. In the case of amine-treated silica nanoparticles, a strongly water-wet condition was not achieved. Oil displacement experiments confirmed the better performance of amine-surfactant-treated SiO₂ nanoparticles compared to amine-treated SiO₂ by improving oil recovery by 15%. Overall, a synergistic effect between Azarboo surfactant and amine-modified silica nanoparticles led to wettability alteration and higher oil recovery.



Citation: Khoramian, R.; Kharrat, R.; Pourafshary, P.; Golshokoh, S.; Hashemi, F. Spontaneous Imbibition Oil Recovery by Natural Surfactant/Nanofluid: An Experimental and Theoretical Study. *Nanomaterials* **2022**, *12*, 3563. <https://doi.org/10.3390/nano12203563>

Academic Editor: Ana María Díez-Pascual

Received: 19 September 2022

Accepted: 5 October 2022

Published: 12 October 2022

Publisher's Note: MDPI stays neutral with regard to jurisdictional claims in published maps and institutional affiliations.



Copyright: © 2022 by the authors. Licensee MDPI, Basel, Switzerland. This article is an open access article distributed under the terms and conditions of the Creative Commons Attribution (CC BY) license (<https://creativecommons.org/licenses/by/4.0/>).

Keywords: natural surfactant; nanoparticles; spontaneous imbibition; mathematical modeling; enhanced oil recovery

1. Introduction

Oil recoveries have declined in many oil fields worldwide [1]. Different chemical and physical techniques have improved oil recovery [2,3]. Wettability alteration is an effective mechanism that results in higher oil recovery [4,5]. Nanoparticles are proposed as efficient wettability modifiers during oil extraction [6]. Destabilization under harsh conditions of reservoirs has led researchers to modify nanoparticles with different surfactant agents [7].

Even though the role of surfactants in oil reservoirs is mainly to modify the wetting condition of oil-wet rocks and reduce the interfacial tension (IFT), they can also disperse or stabilize nanoparticles [8]. Nwidee et al. [9] showed that the functional ZrO₂ nanoparticles facilitated wettability alteration by adsorption on the rock surface, confirmed by microscopic images and contact angle measurements. Imbibition tests revealed a fast water imbibition process for the rock samples coated with the surfactant-modified nanofluid. Rezk and Allam [10] unveiled the synergetic effect of sodium dodecylbenzene sulfonate (SDBS) anionic surfactant and zinc oxide (ZnO) nanoparticles on interfacial tension, wettability,

and oil productivity. A remarkable decrease in the interfacial tension was observed upon adding ZnO nanoparticles into the surfactant solution and attributed to the nanoparticles' low polydispersity and uniformity. The ZnO-based nanofluid, overcoming the capillary pressure, altered wettability to further water wet state and improved oil recovery by 8%. Zhao et al. [11] combined a nonionic surfactant and SiO₂ nanoparticles for EOR applications. Imbibition studies showed higher oil recovery than the standalone application of nanofluid or surfactant. Soleimani et al. [12] synthesized ZnO nanoparticles via the sol-gel method and dispersed them in the aqueous phase using sodium dodecyl sulfate (SDS). The highest oil recovery was observed at 3000 ppm ZnO due to interfacial tension and wettability alteration. Divandari et al. [13] coated magnetic nanoparticles with a surfactant and proved better wettability alteration and lower precipitation.

Cetyltrimethylammonium bromide (CTAB) is a typical cationic surfactant with long-chain carbons, which bears positive charges on the polar portion of fluids [14]. Ma et al. [15] studied surface modification of silica nanoparticles with CTAB nanoparticles at different temperatures and concentrations. Due to the positive charges of CTAB and negative charges of SiO₂, the CTAB could be absorbed on the surface of nanoparticles and improve the dispersal state of the nanoparticles. Using sand column experiments, Liu et al. [16] observed better transport and retention of graphene oxide nanosheets dispersed in CTAB and SDBS. Panahpoori et al. [17] improved CTAB foam stability at harsh reservoir conditions using TiO₂ nanoparticles. Pereira et al. [18] modified the surface of Fe₃O₄ nanoparticles using CTAB. The resultant nanoparticles were stable even in divalent cations and more capable of altering the rock wettability. Joshi et al. [19] investigated using SiO₂ with polymers and CTAB surfactants to increase the oil recovery from oil reservoirs. The stability of nanofluids was improved when surfactant agents were utilized. Synergistic effects of polymer, nanoparticle, and surfactant contributed to IFT reduction, wettability alteration, and viscosity enhancement. Hethnawi et al. [20] studied the interfacial behavior of CTAB-grafted faujasite-based nanoparticles under various conditions. The developed nanofluid showed a considerable improvement in IFT and viscoelasticity.

The published EOR studies have focused on nanofluids combined with synthetic surfactants like CTAB, SDBS, and SDS, which are known to be toxic aquatic organisms [21]. Recent international regulations prohibit using non-biodegradable and toxic chemicals [22], which contributes to phasing out some surfactant agents. To address this challenge, researchers' focus has shifted to new non-toxic alternatives for petrochemical surfactants. Nowrouzi et al. [23] prepared a non-petrochemical surfactant from powder leaves of *Myrtus communis*, a source of natural surfactants. The surfactant increased oil recovery by 14.3% and reduced IFT to 0.86 mN/m and had low adsorption on the rock surface. Khayati et al. [24] found pure saponin very effective for IFT reduction and wettability alteration to hydrophilicity. Emadi et al. [25] investigated the impact of foam generated by Cedar extract on mobility control and introduced it as an advisable chemical agent for EOR. Pa et al. [26] fabricated sunflower Gemini surfactants, leading to stable emulsions, ultralow IFT, and great foamability. Traiwiriyawong et al. [27] extracted a benign surfactant from palm kernel oil and used it in wettability studies. It showed the least adsorption compared to commercial surfactants of SDS and CTAB.

Recently, amine molecules have been used for surface modification of nanoparticles rather than chemical surfactants. Wang et al. [28] aminated SiO₂ nanoparticles with tris(hydroxymethyl)aminomethane and steric acid to increase hydrophobicity. The contact angle of SiO₂ was initially around 18° due to several hydroxyl groups on the SiO₂ surface, but it increased by almost 100° after amination, implying high hydrophilicity of aminated nanoparticles. Habibi et al. [29] utilized amines and organosiloxane for homogenized dispersibility and surface modification of SiO₂ nanoparticles. The surface modification remarkably improved wettability and surface activity, resulting in higher oil recovery in micromodel floodings. In another study [30], aminobutanol was utilized to improve the surface activity of SiO₂ nanoparticles by amination. The reactivity of the nanoparticles was increased and enabled them to be grafted more easily to carboxylic acids.

This study aims to amine SiO_2 nanoparticles and combine them with a new green natural surfactant from bio-sources called Azarboo (Chooback). Hence, SiO_2 nanoparticles are first modified with positively charged amine groups to become ready to absorb Azarboo anionic surfactant (Figure 1). The performance of this new chemical is experimentally studied in this work. The experimental results are then analyzed using the capillary number and validated by the analytical approach by Mattax and Kyte [31], Ma et al. [32], and Aronofsky et al. [33].

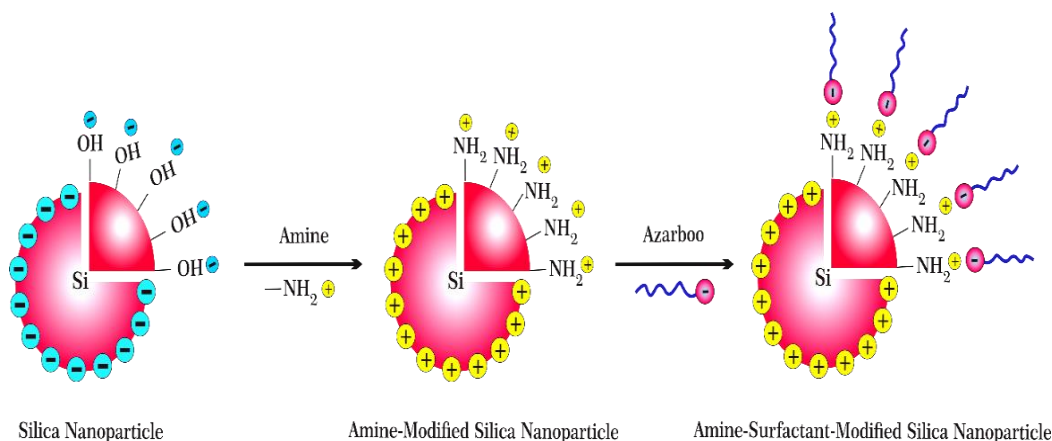


Figure 1. Amine and surfactant modification of silica nanoparticles using Azarboo and amine molecules.

2. Experimental Section

2.1. Materials

The natural surfactant powder of Azarboo (Chooback) was utilized in this study. This green surfactant was extracted from hard and bony roots of *Acanthophyllum*, which has a bitter taste and yellow color. Due to having hydrophilic and hydrophobic parts at the same time, it can create thick and stable foams [34].

Hydrophilic colloidal silicon oxide nanoparticles were utilized in this investigation with a purity of >99.9 wt.%. The mean particle size of the nanomaterials was between 5 and 15 nm. Different chemical and physical characteristics of the nanoparticles are shown in Table 1.

Table 1. The physical and chemical properties of the silica nanoparticles.

Nanoparticle	Color	Shape	Average Size	pH	Density (g/cc)	Surface Area (m^2/g)
SiO_2	White	Spherical	5–15	3.7–4.7	5×10^{-2}	200

Carbonate core samples of 3.8 cm in diameter and 6.5 cm in length were utilized in wettability alteration and core flooding experiments. Table 2 shows the properties of core samples. Two slices with 3 mm thickness were cut from one of the core plugs and polished to be smooth enough for contact angle experiments.

Table 2. The physical characteristics of the carbonate samples utilized in this survey.

Core No.	Permeability	Porosity	Diameter	Length	Pore Volume	S_{wir} (Irreducible Water Saturation)
1	48.3 mD	21.6%	3.82 cm	6.72 cm	16.6 cc	29.5
2	52.7 mD	19.2%	3.87 cm	6.39 cm	14.4 cc	28.3
3	54.7 mD	19.8%	3.81 cm	6.48 cm	14.6 cc	26.3
4	49.3 mD	18.5%	3.85 cm	6.53 cm	14.1 cc	30.1

Ethanol (99%) and 3-aminopropyltriethoxysilane (APTS) were from Merck Company (Darmstadt, Germany). The chemical composition and properties of the degassed oil used in this study are also listed in Table 3.

Table 3. The oil properties and composition at 14.7 psi and 60° F.

Chemical Properties	Value
C ₁	0.08 mole%
C ₂	0.14 mole%
C ₃	1.48 mole%
iC ₄	1.06 mole%
nC ₄	4.65 mole%
iC ₅	2.69 mole%
nC ₅	1.29 mole%
C ₆	8.23 mole%
C ₇₊	80.38 mole%
Gravity	36.8° API
Density	0.823 g/cc
Viscosity	23.9 cp

2.2. Methodology

2.2.1. Amine Functionalization

Amine functionalized silica nanoparticles were prepared using the reaction of silica nanoparticles and APTS at room temperature. 1 mL APTS was dissolved into 200 mL ethanol in a beaker on a stirrer. Then, 10 g silica nanoparticle was added to the beaker and sonicated for 1 h. It was followed by adding 150 mL distilled water to the mixture and sonication for half an hour. The mixture was centrifuged under 15,000 rpm for almost 20 min, and the precipitated part was collected and washed with ethanol. Amino-modified silica nanoparticles (Si-NH₂) were obtained by gently heating the gel-like precipitation at 50 °C for 6 h [35].

2.2.2. Natural Surfactant Extraction and Optimization

The maceration procedure [36] was used to get the *Acanthophyllum* plant extract. The bony roots of this plant were dried at ambient temperature and pulverized using an electric mortar and pestle. Then, almost 400 g of the dried plant powder was combined with distilled and kept in a sealed Erlenmeyer flask for at least three days. The Erlenmeyer flask was shaken using an orbital shaker to mix the powder with water continually. The flask's contents were then filtrated and transferred into a digital rotary evaporator flask (DLAB) for about five hours to obtain a dry extract powder (Figure 2).

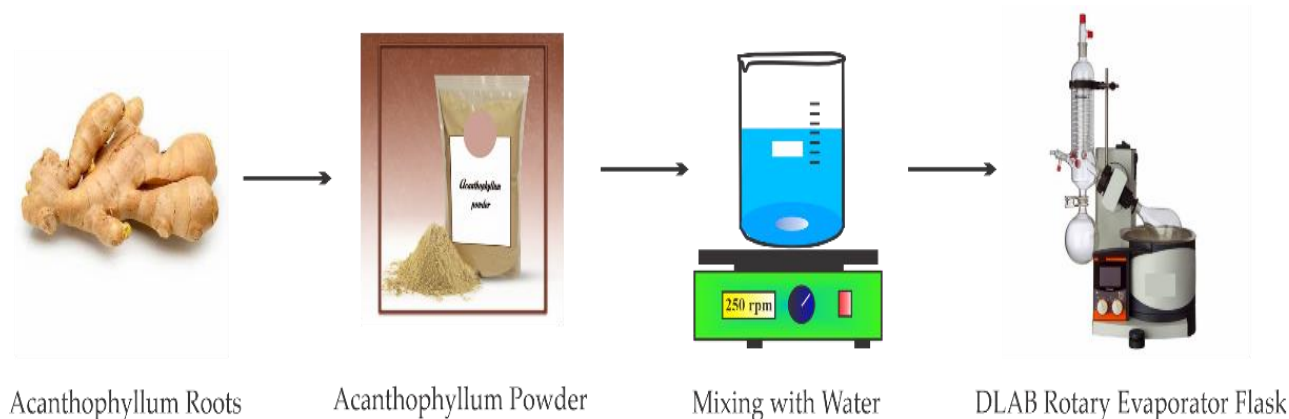


Figure 2. Experimental procedures used in preparing the Azarboo Surfactant.

Surfactant solutions were prepared at different concentrations (200–2000 ppm) by combining the extracted Azarboo and synthetic brine (180,000 ppm NaCl) on a magnetic

stirrer for 10 min. Then, electrical conductivity and IFT were measured to find the surfactant's critical micelle concentration (CMC). The IFT and conductivity values were recorded versus concentration (Figure 3), and CMC was found at 1200 ppm. No further tests were done beyond this threshold, as the IFT does not change after the CMC value [37,38].

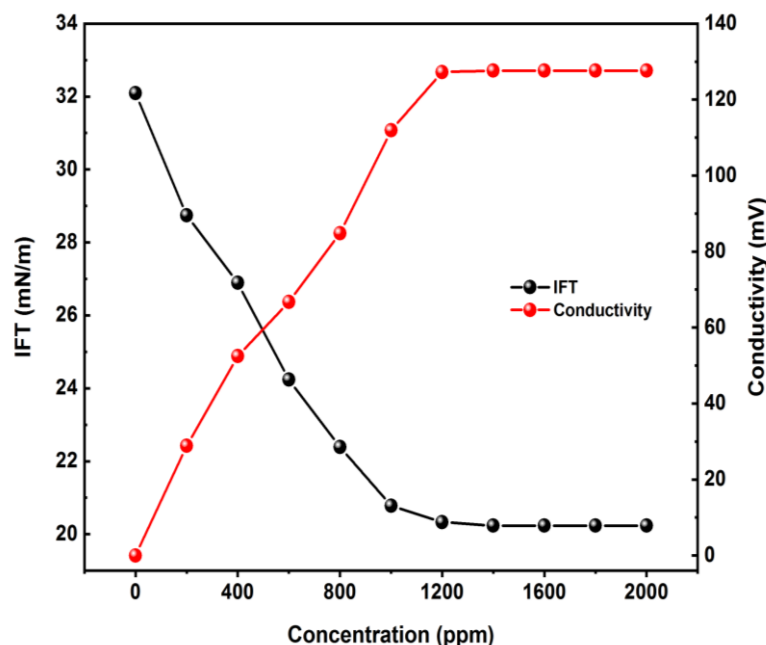


Figure 3. Surface conductivity and IFT versus Azarboo concentration for CMC determination.

Measurements showed an almost 39% decrease in IFT (Figure 3), which confirmed a very good influence of the natural surfactant on emulsification and IFT reduction, which is considered as effective EOR mechanisms.

2.2.3. Surfactant/Nanofluid Preparation

It has been proven that nanoparticles can penetrate the micron-sized pores and throats of the reservoir rocks and improve oil recovery afterward [39,40]. The nanoparticles can unfavorably affect fluid flow in the porous media if the nanofluid concentration exceeds a certain amount due to entrapment [41,42]. Hence, a concentration of 500 ppm of the Si-NH₂ nanoparticles was selected and applied to prepare Azarboo/nanofluid. The concentration had been introduced by extensive research for various nanoparticles [43,44]. The Azarboo/nanofluid was prepared by dispersing 500 ppm of the modified nanoparticles into the surfactant solution (1200 ppm surfactant with 180,000 ppm NaCl). To better evaluate the properties of the developed nanofluid, samples without the natural surfactant (pure silica and Si-NH₂) were also prepared. The nanofluids were softly stirred for two hours (one hour with an ultrasonic probe and one hour inside an ultrasonic bath) at 20 kHz. The objective was to utterly suspend the nanoparticles into the dispersion medium and prevent aggregation.

2.2.4. Surfactant Characterizations

Fourier transform infrared (FT-IR) spectrum of Azarboo was recorded on a PerkinElmer Spectrum™ 3 FT-IR spectrometer (Waltham, MA, USA) and compared with those of amine-treated and surfactant-modified nanoparticles for functional analysis. The proton nuclear magnetic resonance (H-NMR) spectroscopy was done using Bruker 500 MHz EPR (Billerica, MA, USA), to determine the structure of Azarboo molecules. The natural surfactant was thermally studied by thermogravimetric analysis (TGA). TGA, which was performed using TGA-Q600 SDT (Milford, CT, USA) is a technique to detect how materials behave when

subjected to heat. Three milligrams of natural surfactant were poured into a crucible and heated to almost 350 °C at a rate of 10 °C/min under a nitrogen atmosphere [45].

The particle size distribution was measured using a dynamic light scattering (DLS) instrument from Malvern Company (Worcestershire, United Kingdom). The Brunauer-Emmett-Teller (BET) technique was utilized to measure the surface areas of silica nanoparticles before and after modification through gas adsorption analysis by a Miraesi KICT-SPA 3000 Instrument (Miraesi, Korea). Scanning electron microscopy (SEM) images were captured using an electron microscope (HITACHI, model SU7000, Tokyo, Japan) to study nanoparticles' morphology. The average zeta potential values of the nanoparticles were measured using a zeta potential analyzer (ZEECOM ZC2000ML Microtec Company, Brixen, Italy) at 25 °C. The zeta potential values were recorded by averaging three zeta potential measurements for each sample based on previous studies [46,47]

2.2.5. Oil-Wet Procedure

All samples were saturated and soaked in crude oil at 50 °C for three weeks to be oil-wet before imbibition experiments. After aging, they were found entirely oil-wet due to having contact angles lower than almost 150° and color change from gray to dark brown (Figure 4).

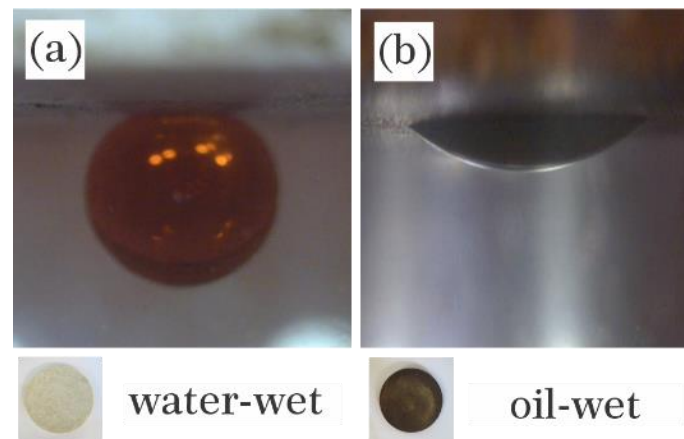


Figure 4. Images of carbonate thin sections (a) before and (b) after aging in crude oil correspond contact angles.

2.2.6. Spontaneous Imbibition

The spontaneous imbibition test [48] was used to assess the wetting condition of the rocks qualitatively. Two core plugs (No. 1 and 2) with induced oleophilic wettability were drenched in the prepared nanofluids for 24 h at room temperature. Each sample was taken out and dried at 40 °C for one day. They were saturated with oil and placed inside brine-filled Amott cells at 50 °C. The volume of oil expelled was measured by monitoring the graduation of the cell [49]. Another imbibition test was conducted with an oil-wet sample without treatment with nanofluids.

Mattax and Kyte [31] proposed a scaling group for imbibition oil recovery from strongly water-wet systems with distinct rock and fluid characteristics as

$$t_D = \left(\frac{0.00031415}{L_C^2} \sqrt{\frac{k}{\phi} \frac{\sigma_{ow}}{\mu_o \mu_w}} \right) t \quad (1)$$

where t_D is a dimensionless time, L_C is a characteristic length (cm), k is permeability (mD), ϕ is porosity, σ_{ow} is oil-water interfacial tension (dyne/cm), μ_o is oil viscosity (cp), μ_w is

water viscosity (cp), and t is the imbibition time (hr.). Ma et al. [32] developed a single-parameter model, which was a simplified form of the Aronofsky et al. [33] model as

$$\frac{R}{R_{Max}} = 1 - e^{-\alpha t_D} \quad (2)$$

where R is imbibition oil recovery, R_{Max} is ultimate oil recovery by free imbibition, and α is the decline constant of oil production.

2.2.7. Core Flooding Experiments

Displacement experiments were performed using a core flood apparatus shown in Figure 5. Cores No. 3 and 4, previously aged to become oil-wet, were selected for this section. The core plugs were washed and cleaned with toluene, methanol, and distilled water using the Soxhlet extractor to remove any dirt. Then they were heated in a furnace at almost 100 °C for 24 h to be dried [50]. The cores were saturated by a brine of 180,000 ppm NaCl. Oil was injected until no additional brine was expelled from the cores and irreducible water saturation was established. After that, the synthetic brine was flooded into the cores to mimic the secondary oil recovery. One pore volume of pure Si-NH₂ and Si-NH₂ modified with Azarboo was then injected into the core plugs as the tertiary oil recovery stage. The injection was stopped, and the core was soaked in the nanofluids for 24 h to alter the pores' wettability [51]. After the shut-in treatment, the cores were fully saturated with the brine and then with the oil until the irreducible water saturation was established. This stage aimed to monitor oil recovery after the nanofluid treatment. In the flooding tests, the temperature was 50 °C, the flow rate was 0.1 cc/min, and the radial confining pressure was almost 500 psi higher than the injection pressure.

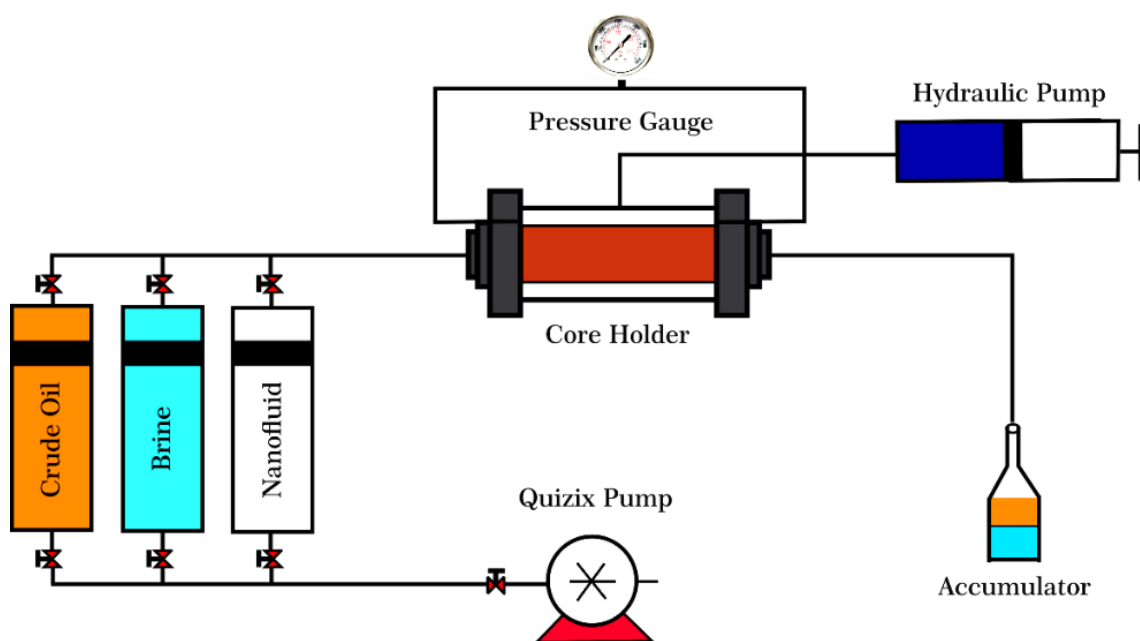


Figure 5. A schematic illustration of the core flooding setup.

3. Results and Discussions

3.1. Characterization Results

3.1.1. Natural Surfactant

The functional groups and chemical compositions of the natural surfactant were studied by FT-IR, H-NMR, and TGA analyses. In the FT-IR spectrum shown in Figure 6a, the peak at 1057 cm⁻¹ is associated with C–O stretching vibration, and the peak at 1323 cm⁻¹ corresponds to the –OH bond [52]. The peak at 1625 cm⁻¹ in the carbonyl stretching region was mainly due to a covalent bond between two carbon atoms (C=C) [34]. Also,

the peak around 2900 cm^{-1} was linked to C–H aliphatic saponin graft [53]. Commonly, intense broadband at $3000\text{--}3600\text{ cm}^{-1}$ area can be seen in the IR spectrum of polysaccharides [54]. This strong band, which represents the stretching vibration of multiple hydroxyl groups (–OH) in polysaccharides, was observed at 3418 cm^{-1} . These characteristic functional groups exist in the structure of Azarboo surfactant.

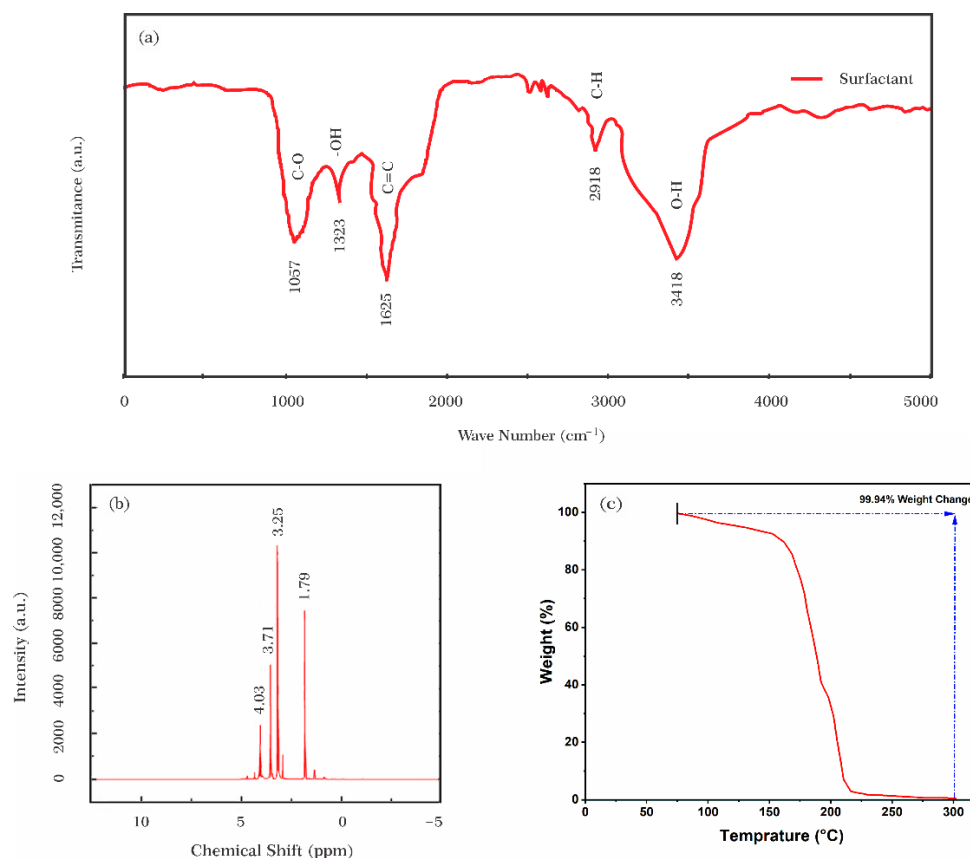


Figure 6. (a) FT-IR spectrum (b) $^1\text{H-NMR}$ spectrum and (c) TGA analysis of Azarboo surfactant.

In the $^1\text{H-NMR}$ spectrum, different chemical peaks were observed as shown in Figure 6b. The peak at about 4 ppm corresponds to the hydroxylic group (–OH). The chemical shifts from 2.8 to 3.8 ppm are related to the saponin oligosaccharide functional group, and those between 1.5 and 2.5 ppm are attributed to the glycoside-free aglycone section of the saponin [34]. These results were consistent with the presence of the FT-IR bands at 1057 cm^{-1} , 2900 cm^{-1} , and 3418 cm^{-1} , as discussed above.

TGA analysis for Azarboo surfactant was performed under a nitrogen atmosphere. As illustrated in Figure 6c, the natural surfactant was thermally fully stable up to about $75\text{ }^{\circ}\text{C}$, beyond which the weight loss initiated and steadily continued to $160\text{ }^{\circ}\text{C}$. A probable reason for that weight loss is water evaporation from molecules and particles [55]. The thermal stability of the surfactant followed the decreasing trend more steeply, reaching $300\text{ }^{\circ}\text{C}$, where only less than 1% of the natural surfactant remained unchanged. This heavyweight loss, which is due to carbon bond breakdown at high temperatures [56], reveals that Azarboo is natural and extracted from plants [57]. In conclusion, TGA analysis confirms the thermal usability of the Azarboo surfactant for harsh-temperature EOR operations due to great mass maintenance at temperatures below $100\text{ }^{\circ}\text{C}$.

3.1.2. Aminated Silica Nanoparticles

FT-IR analysis was used to indicate amine modifications on SiO_2 nanoparticles. Figure 7 shows the IR spectrum of silica nanoparticles before and after modification. Looking at the FT-IR spectroscopy of silica nanoparticles (Figure 7, red line), the bands

at 779 and 1097 cm^{-1} are attributed to bending vibration or asymmetric stretching vibration of Si–O–Si bonds [58]. The absorption bands at 1583 and 3490 cm^{-1} are assigned to O–H stretching [59]. The Si-NH₂ nanoparticles were detected through new peaks in IR spectra (Figure 7, blue line). The new bands at 1562 and 1716 cm^{-1} originate from amine groups' N–H bending vibration [58]. Also, the broad and strong band at 3477 cm^{-1} may be attributed to the substitution of –OH stretching with the N–H stretch of amine [60]. All these observations represent that amine-functionalized silica nanoparticles have been synthesized successfully.

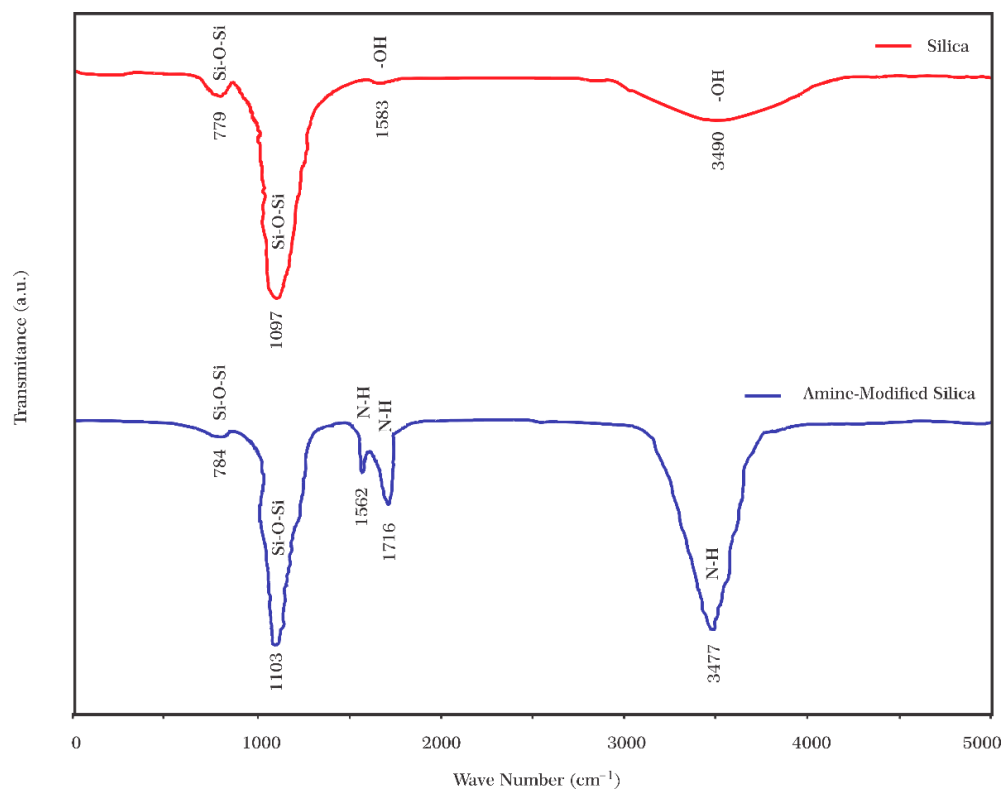


Figure 7. FT-IR spectrums of bare and amine-modified SiO₂ nanoparticles.

The zeta potential of bare and Si-NH₂ nanoparticles was measured to confirm the N–H conjugation on the surface. Bare SiO₂ nanoparticles were quantified as a control, which indicated a negative zeta potential (−25 mV). Contrarily, the zeta potential for Si-NH₂ nanoparticles was positive (+21 mV). As silica nanoparticles are filled with negative charges, and amino groups are replete with positive ones, it is evident that amine functionalization has been done efficiently (see Figure 1).

3.1.3. Amino-Surfactant-Modified Silica Nanoparticles

The linkage of Azarboo surfactant to Si-NH₂ nanoparticles was investigated by FT-IR spectroscopy. The IR spectrum of the surfactant was measured as a control (Figure 6a) to identify new functional groups in amino surfactant nanocomposite (Si-NH₂-surfactant) after surfactant modification (Figure 8a). The results showed that all functional groups observed in Azarboo surfactant molecules appeared in IR spectroscopy of Si-NH₂-surfactant. In addition, a weak peak at 792 cm^{-1} showed the bending vibration of Si–O–Si bonds, and a sharp peak at 1723 cm^{-1} represented the vibration of N–H. As evidenced in Figure 8, it is proven that Azarboo surfactants are linked to Si-NH₂ nanoparticles.

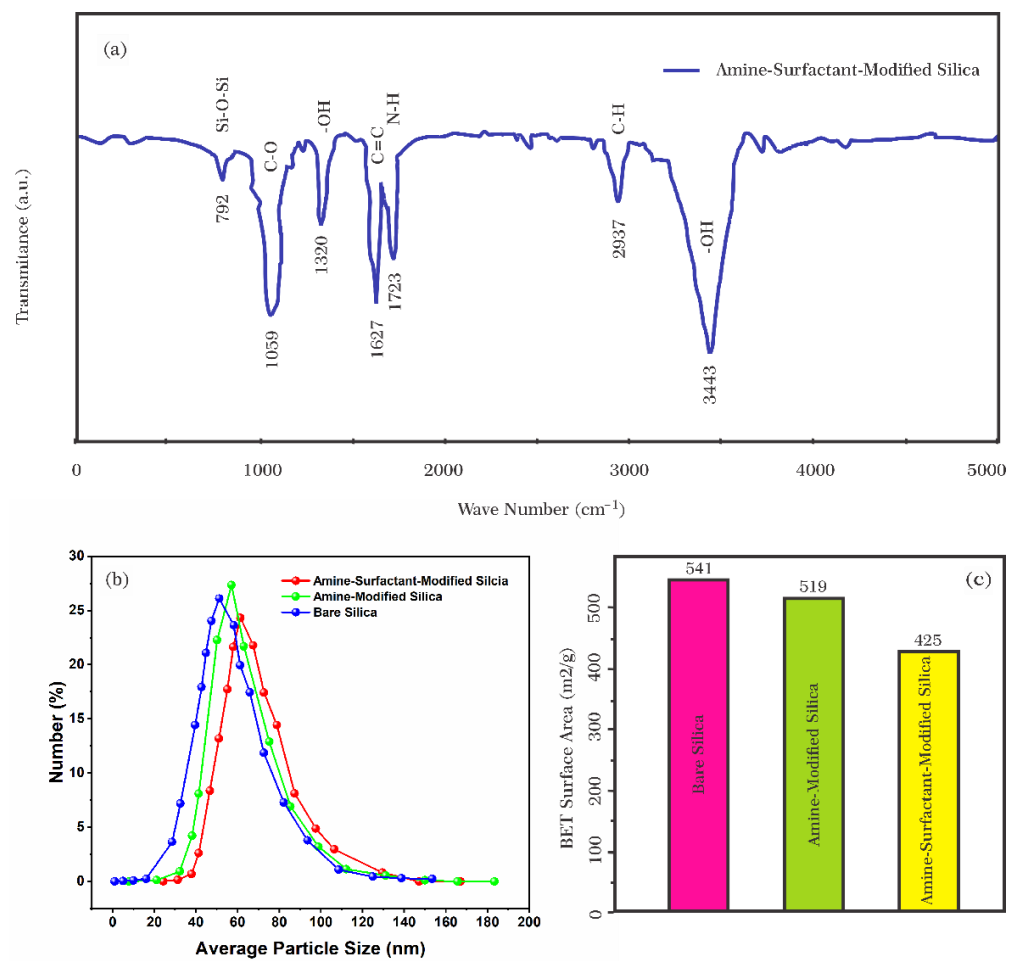


Figure 8. (a) FT-IR spectrum of amine-surfactant-modified SiO₂ nanoparticles, (b) particle size distribution and (c) BET surface area of bare, amine-treated, and amine-surfactant-treated SiO₂ nanoparticles.

The zeta potential of Si-NH₂-surfactant nanoparticles was also recorded. The zeta potential reached a negative value (−17 mV) from a positive value (+21 mV). It confirmed surfactant conjugation on positively charged aminated silica nanoparticles (see Figure 1). In addition, the hydrodynamic diameter of the particles in the nanofluid was measured at a constant concentration of 500 ppm Si-NH₂ nanoparticles with and without 1200 ppm Azarboo surfactant in distilled water. The results demonstrated two narrow bell-shaped size distributions ranging from 20 nm to 140 nm (Figure 8b). The average size of 57 nm was measured for Si-NH₂, being higher than that of bare SiO₂. The size was increased by about 5 nm and reached 62 nm after treatment with surfactant. The size change is due to the linkage of the Azarboo surfactant. Taking negative charges on the Azarboo surfactant into account, it could be conjugated on the surface of positively charged Si-NH₂ nanoparticles using electrostatic forces. Thus, Si-NH₂-surfactant nanoparticles would have a larger particle size, which is consistent with other studies [59].

The presence of Chooback surfactant in the structure of SiO₂ nanoparticles was further studied by measuring the BET surface area before and after treatment with amine and surfactant. As shown in Figure 8c, bare SiO₂ nanoparticles had a higher BET surface area than aminated and surfactant-modified nanoparticles (541 m²/g versus 519 m²/g and 425 m²/g). Chooback molecules could be adsorbed on SiO₂ nanoparticles and modify their surfaces [15,61]. This result was confirmed using SEM images with a scale of 10 nm (Figure 9). SiO₂ nanoparticles before treatment were round and spherical, with an average size of almost 5–10 nm (Figure 9a). However, after treatment with Chooback, they became foamy, whiter, and larger (Figure 9c), which confirms the surface modification. In contrast,

no sensible change was observed in the form of SiO₂ nanoparticles after amination, and they became only a bit whiter (Figure 9b).

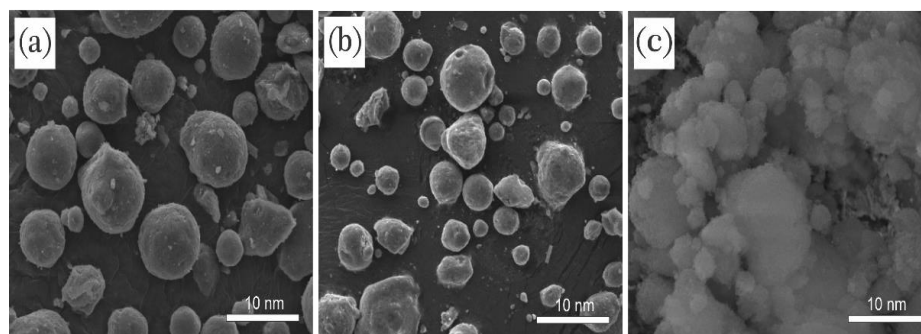


Figure 9. SEM images of (a) bare, (b) aminated, and (c) amine-surfactant-treated silica nanoparticles with a 10-nm scale.

3.2. The Effect of the Nanoparticle on Wettability

The natural surfactant of Azarboo and amine molecules were utilized for the surface modification of SiO₂ nanoparticles. The modification was proven using different characterization tests. Herein, the performance of the developed nanofluid is studied for wettability alteration using spontaneous imbibition and surface imaging technique.

3.2.1. Spontaneous Imbibition

Spontaneous imbibition occurs when a wetting fluid displaces a non-wetting fluid in porous media without external forces [62,63]. Three oil-wet carbonate samples were employed to know how Si-NH₂ and Si-NH₂-surfactant would affect the spontaneous imbibition oil recovery. Figure 10 demonstrates the oil recovery results for the samples after almost two months. As can be seen, the oil-wet sample had the lowest imbibition with an oil recovery of 14%, proving its oil-wet tendency. The amount of oil produced after modification with Si-NH₂ was around 23%, and after treatment with Si-NH₂-surfactant was about 28%. It was evident that almost 14% and 9% of the oil recovered should have been due to Si-NH₂-surfactant and Si-NH₂ nanoparticles. Even though the rate of oil production was noticeably higher when Si-NH₂-surfactant was applied. So, this test is evidence of wettability alteration by the modified chemicals.

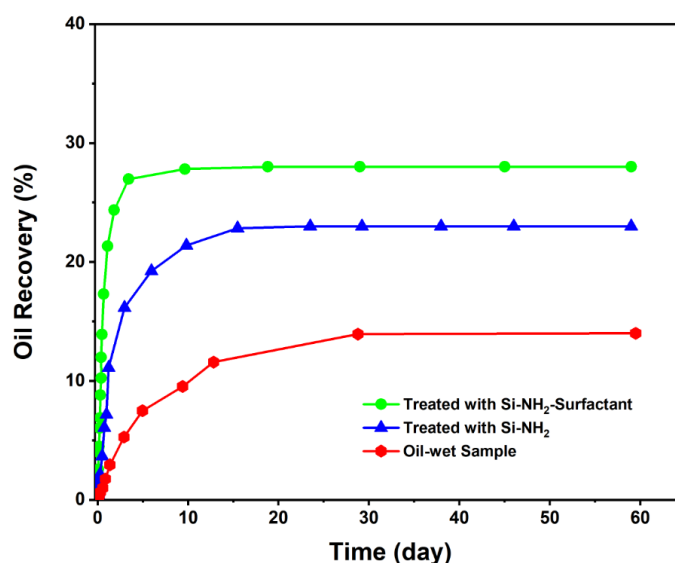


Figure 10. Spontaneous imbibition oil recoveries of the oil-wet sample, and core plugs treated with Si-NH₂-surfactant and Si-NH₂ nanofluids.

3.2.2. Surface Imaging

In the previous section, both Si-NH₂-surfactant and Si-NH₂ nanoparticles were hydrophilic, but different oil recoveries were obtained. A surface imaging technique was employed to visualize the alterations originating from nanoparticle obstruction. Each of the core plugs was cut horizontally and split in two. Then, SEM photographs were taken before and after exposure to Si-NH₂-surfactant and Si-NH₂ nanofluids (Figure 11).

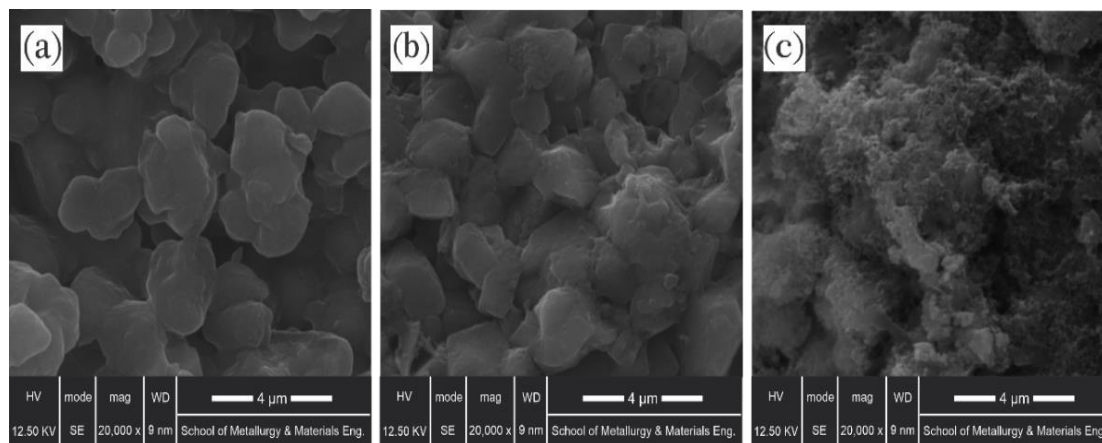


Figure 11. SEM images of the rock samples, (a) soaked in crude oil, (b) treated with Si-NH₂, and (c) drenched in Si-NH₂-surfactant.

Figure 11a illustrates the morphology of the oleophilic media before treatment with nanofluid, and Figure 11b,c shows the oil-wet slice morphology after treatment with Si-NH₂ and Si-NH₂-surfactant, respectively. The rock sample soaked in oil (Figure 11a) has roughened a little after exposure to Si-NH₂ nanofluid, as shown in Figure 11b. This roughness is because of the low-affinity adsorption of Si-NH₂ nanoparticles on the carbonate surface. In contrast, Figure 11a,c showed that Si-NH₂-surfactant nanoparticles had substantially adsorbed over the cleaned porous medium. Compared to treatment with Si-NH₂, the open and visible pores had become closed and invisible, offering Si-NH₂-surfactant nanoparticles further interacting with the oil-wet carbonate samples.

Surface roughness is a critical factor that affects wettability. Contact angles were also measured to confirm the nanoparticles' adsorption. Angles were recorded after aging rock surfaces in oil, Si-NH₂, and Si-NH₂-surfactant nanofluids (Figure 12a). The contact angle for the oil-wet rock chip was 147°, confirming an initial oleophilic condition. Contact angles for Si-NH₂-surfactant and Si-NH₂ nanofluids were changed to 36° and 85°, respectively. Hence, amine-treated nanoparticles changed the wetting state to neutral-wet and surfactant-treated nanoparticles to strongly water-wet.

Rostami [64] stated the hydrophilic property of silica nanoparticles as the reason for changing the wetting condition to water-wetness. Khoramian et al. [65,66] showed the amphiphilic nature of graphene oxide nanosheets for restoring wettability to mixed-wetness. Thus, wettability alteration to a more water-wet state and change in surface roughness are because of the attraction between heavy oil compositions deposited on the rock surface and the hydrophobic tail of the natural surfactant in the Si-NH₂-surfactant (Figure 12b). It, in turn, contributed to higher adsorption of Si-NH₂-surfactant nanoparticles and water-wet wettability alteration.

The scaling approach was utilized to magnify the difference in imbibition oil recovery data [67]. Figure 13 is re-plotted where $R_D = \frac{R(t)}{R_T}$ and $R(t)$ is oil recovery at different times, and R_T is the final oil recovery. Hence, the x -axis shows imbibition duration, and the y -axis presents the normalized imbibition oil recovery of the core samples. From the results, the surfactant-treated sample (green line) exhibited a very swift imbibition process and reached maximum oil recovery after only nine days due to its hydrophilic

nature ($\theta = 36^\circ$). In contrast, the non-treated oleophilic sample (black line) showed the slowest imbibition rate within twenty-eight days and the highest imbibition resistance. Capillary forces prevent the non-wetting fluid from imbibing in an oil-wet sample, slowing down the imbibition rate [68,69]. The Si-NH₂ treatment could also restore the original wettability and increase the speed of spontaneous imbibition. However, Si-NH₂ treatment permitted a considerable restoration of the rock sample wettability ($\theta = 85^\circ$). The results demonstrated the better effectiveness of the Si-NH₂-surfactant in modifying the wettability and accelerating the process to reach the maximum recovery, nine days versus fifteen days. The results can be clarified more sensibly when they are made dimensionless using the spontaneous imbibition scaling parameters [70,71].

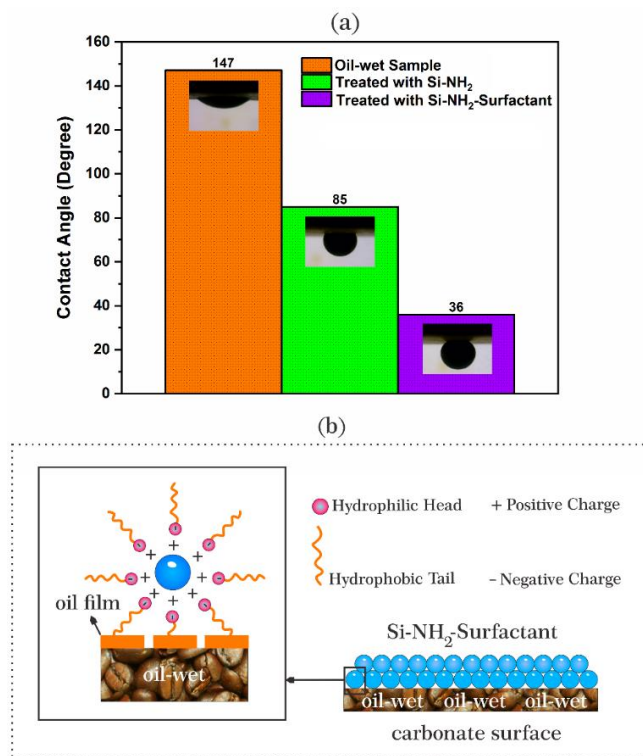


Figure 12. (a) The wetting angle (θ) values for three carbonate rock samples and (b) the representational image of wettability alteration by Si-NH₂-Surfactant nanoparticles.

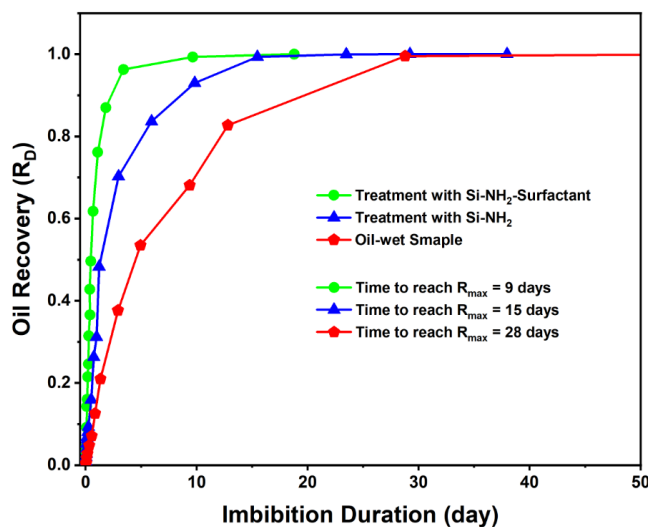


Figure 13. Normalized spontaneous imbibition curves for the three tests.

Herein, the scaling group of Mattax and Kyte [31] was utilized to calculate t_D based on the parameters listed in Table 4 for analytical comparisons of the results.

Table 4. The characteristics of the carbonate samples and fluids used in spontaneous imbibition experiments.

Parameter	Oil-Wet Sample	Aminated Sample	Surfactant-Amine-Treated Sample
Permeability (mD)	52.7	48.3	52.7
Porosity (%)	19.2	21.6	19.2
Length (cm)	6.39	6.72	6.39
Water Viscosity (cp)	0.97	1.07	1.03
Oil Viscosity (cp)	23.9	23.9	23.9
Interfacial Tension (dyne/cm)	32	20	30
$t_D = \left(\frac{0.00031415}{L_{c2}^2} \sqrt{\frac{k}{\phi}} \frac{\sigma_{ow}}{\sqrt{\mu_o \mu_w}} \right) t$	$t_D = 0.051 \text{ t (hr.)}$	$t_D = 0.025 \text{ t (hr.)}$	$t_D = 0.046 \text{ t (hr.)}$

To estimate α , dimensionless imbibition oil recovery was plotted versus dimensionless time for all tests based on the model developed by Ma et al. [32] (Figure 14). Mattax and Kyte [31] showed that a constant production decline of 0.05 is devoted to strongly water-wet systems. If $\alpha < 0.05$, then the system becomes less water wet. In our study, the oil-wet sample α is 0.002, which means the least water-wet condition, as expected. The imbibition results of the rock sample treated with Si-NH₂ nanoparticles were fitted with $\alpha = 0.006$, which showed a partially water-wet condition. Results of the case of the Si-NH₂-surfactant nanoparticles matched the decline constant of 0.03, which shows a strongly water-wet porous media [72].

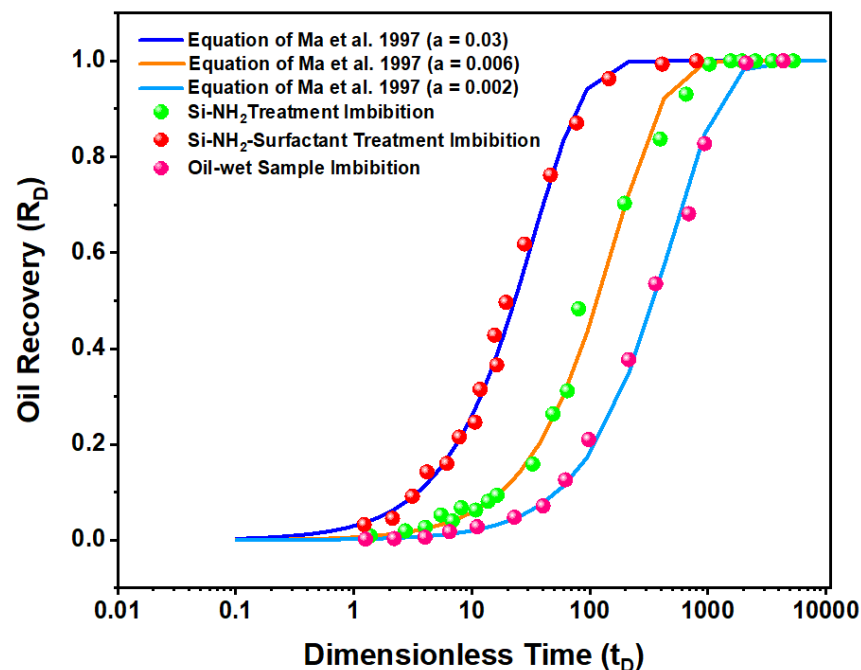


Figure 14. Imbibition oil recovery versus dimensionless time for the oil-wet sample and samples treated with Si-NH₂-surfactant and Si-NH₂ nanofluids. All tests are based on the model developed by Ma et al. 1997.

Three different alpha values indicated three different imbibition rates and wettability types. A not strongly water-wet system (Si-NH₂) exhibited spontaneous imbibition but with lower imbibition rates. The rate of wettability alteration for surfactant-treated nanofluid was faster, and the process happened sooner. In conclusion, the proposed natural surfactant-based nanofluid can be promising for EOR operations due to higher and faster recovery rates. Thus, it was used for oil displacement and present core flooding.

3.3. Core Flooding

Samples 3 and 4 were soaked in oil and made oleophilic for core flooding experiments. The secondary water flooding was done by injecting six pore volumes of brine with 180,000 NaCl. As shown in Figure 15, only 42 and 45% of the oil was recovered by water flooding. In other words, more than half of the original oil in place was left intact inside the core samples. This low and unfavorable oil recovery was anticipated to the oil-wetness of the rock samples. It was persuasive enough to inject a one-pore volume of Si-NH₂-surfactant and Si-NH₂ nanofluids into cores No. 3 and 4 and allow them to be exposed to the nanoparticles for 24 h. This treatment was done to modify the wettability of the cores toward less oil-wetness. The cores were then saturated with oil until S_{wir} was attained. When the 24-h nano treatment was finished, the second brine flooding was conducted, and the volume of oil recovered was recorded (Figure 15). The second flooding resulted in an oil recovery of 59% for Si-NH₂-surfactant treatment and 49% for Si-NH₂ treatment, showing a surpassing effect of Si-NH₂-surfactant nanoparticles on enhancing oil recovery compared with Si-NH₂. The improvements in oil recovery is due to the wettability restoration and IFT reduction caused by the nanoparticles. The presence of surfactant-treated nanoparticles in the base fluid led to a decrease in interfacial tension from 32 to 20 dyne/cm. This result, which is in a good agreement with previous studies [73], is due to the connection between the hydrophobic head of Azarboo surfactant and crude oil molecules [74].

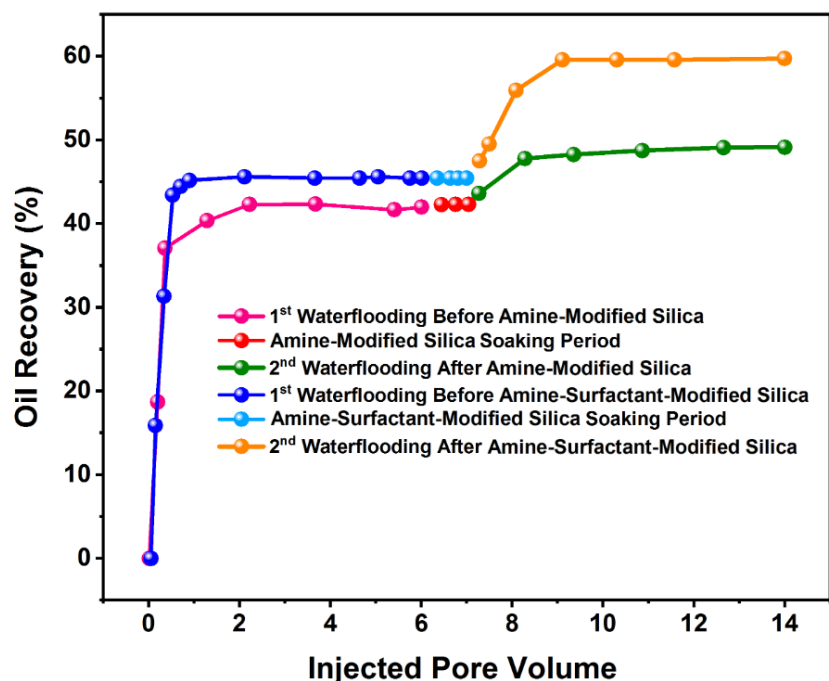


Figure 15. Oil recovery values before and after treatment with Si-NH₂ and Si-NH₂-surfactant nanofluids.

The primary water flooding was run when capillary pressure was negatively high due to the oil-wet inclination of the porous media. Therefore, only wide pores were depleted by water, and a considerable value of oil was trapped inside narrow pores. Aging by the nanoparticles led to the moderate and strong adsorption of Si-NH₂ and Si-NH₂-surfactant on the carbonate media pores and throats, restoring the wettability and decreasing the negative capillary pressure. It, in turn, reinforced water suction into the narrow and small pores and promoted oil recovery to different degrees.

4. Conclusions

A non-toxic anionic surfactant, Azarboo, was obtained from the bony roots of *Acanthophyllum* for possible EOR applications. It was conjugated to positively charged amine-treated SiO₂ nanoparticles and characterized using FT-IR, Zeta potential, DLS, BET, and

SEM analyses. Then, the effects of Si-NH₂ and Si-NH₂-surfactant nanoparticles on the spontaneous imbibition of strongly oil-wet carbonate rocks were experimentally and theoretically examined.

Imbibition results proved the active role of Si-NH₂ and Si-NH₂-surfactant nanoparticles. Maximum oil recovery for treatment with Si-NH₂-surfactant and Si-NH₂ was achieved after nine and fifteen days, respectively, while this result for an oil-wet sample was obtained after twenty-eight days. The rate of wettability alteration was found faster by silica and surfactant together, which was supported by SEM images.

The spontaneous imbibition data were scaled using an analytical model. A decline production constant of 0.006 for the Si-NH₂ imbibition test confirmed that it acted like a partially water-wet system. In contrast, the Si-NH₂-surfactant imbibition test proved a nearly strongly water-wet system with a decline production constant of 0.03. The hydrophobic tails of the natural surfactant could link to oil compositions deposited on porous media and speed up oil production by more wettability alteration and IFT reduction.

The results of core flooding experiments showed the effectiveness of Si-NH₂ and Si-NH₂-surfactant nanoparticles for EOR purposes. The oil production rate experienced an increase of about 15% for Si-NH₂-surfactant nanofluid and almost 7% for Si-NH₂ nanofluid. Overall, the hybrid application of the natural surfactant and silica nanoparticles could improve oil production more than the nano-treatment with anionic molecules.

Author Contributions: Conceptualization, R.K. (Reza Khoramian), R.K. (Riyaz Kharrat), P.P. and S.G.; methodology, R.K. (Reza Khoramian), R.K. (Riyaz Kharrat), P.P., S.G. and F.H.; software, R.K. (Reza Khoramian); writing—original draft preparation, R.K. (Reza Khoramian), R.K. (Riyaz Kharrat), P.P., S.G. and F.H.; writing—review and editing, R.K. (Reza Khoramian), R.K. (Riyaz Kharrat) and P.P.; visualization, R.K. (Reza Khoramian); supervision, R.K. (Riyaz Kharrat), P.P.; project administration, R.K. (Riyaz Kharrat) and P.P.; funding acquisition, P.P. All authors have read and agreed to the published version of the manuscript.

Funding: This research was funded by the Nazarbayev University Faculty Development Competitive Research Grants program, grant number 240919FD3928.

Institutional Review Board Statement: Not applicable.

Informed Consent Statement: Not applicable.

Data Availability Statement: The data will be available on request.

Acknowledgments: The authors would like to thank Nazarbayev University for its administrative and technical support.

Conflicts of Interest: The authors declare no conflict of interest.

References

1. Sircar, A.; Rayavarapu, K.; Bist, N.; Yadav, K.; Singh, S. Applications of Nanoparticles in Enhanced Oil Recovery. *Pet. Res.* **2021**, *7*, 77–90. [[CrossRef](#)]
2. Golshokoh, S.; Khoramian, R.; Ramazani, S.A.A. Methods for Fabricating Porous Media with Controllable Characteristics. U.S. Patent 10,137,393, 27 November 2018.
3. Habib, S.H.; Kania, D.; Yunus, R.; Jan, B.H.M.; Biak, D.R.A.; Zakaria, R. Insight into Hydrophobic Interactions Between Methyl Ester Sulfonate (MES) and Polyacrylamide in Alkaline-Surfactant-Polymer (ASP) Flooding. *Korean J. Chem. Eng.* **2021**, *38*, 2353–2364. [[CrossRef](#)]
4. Dordzie, G.; Dejam, M. Enhanced Oil Recovery from Fractured Carbonate Reservoirs Using Nanoparticles with Low Salinity Water and Surfactant: A Review on Experimental and Simulation Studies. *Adv. Colloid Interface Sci.* **2021**, *293*, 102449. [[CrossRef](#)] [[PubMed](#)]
5. Lu, C.; Liu, H.; Zhao, W.; Lu, K.; Liu, Y.; Tian, J.; Tan, X. Experimental Investigation of In-Situ Emulsion Formation to Improve Viscous-Oil Recovery in Steam-Injection Process Assisted by Viscosity Reducer. *SPE J.* **2017**, *22*, 130–137. [[CrossRef](#)]
6. Golshokoh, S.; Ramazani, S.A.A.; Hekmatzadeh, M. Investigating the Effect of Hybrid Silica Nanoparticles-Copolymer on Increasing Oil Recovery in a Three-Dimensional Porous Media. *Sci. Iran.* **2017**, *24*, 3466–3475.
7. Zhou, Y.; Wu, X.; Zhong, X.; Reagen, S.; Zhang, S.; Sun, W.; Pu, H.; Zhao, J.X. Polymer Nanoparticles-Based Nanofluid for Enhanced Oil Recovery at Harsh Formation Conditions. *Fuel* **2020**, *267*, 117251. [[CrossRef](#)]

8. Cortés, H.; Hernández-Parra, H.; Bernal-Chávez, S.A.; Prado-Audelo, M.L.D.; Caballero-Florán, I.H.; Borbolla-Jiménez, F.V.; González-Torres, M.; Magaña, J.J.; Leyva-Gómez, G. Non-ionic Surfactants for Stabilization of Polymeric Nanoparticles for Biomedical Uses. *Materials* **2021**, *14*, 3197. [[CrossRef](#)]
9. Nwidee, L.N.; Lebedev, M.; Barifcani, A.; Sarmadivaleh, M.; Iglauer, S. Wettability Alteration of Oil-Wet Limestone Using Surfactant-Nanoparticle Formulation. *J. Colloid Interface Sci.* **2017**, *504*, 334–345. [[CrossRef](#)]
10. Rezk, M.Y.; Allam, N.K. Unveiling the Synergistic Effect of ZnO Nanoparticles and Surfactant Colloids for Enhanced Oil Recovery. *Colloids Interface Sci. Commun.* **2019**, *29*, 33–39. [[CrossRef](#)]
11. Zhao, M.; Lv, W.; Li, Y.; Dai, C.; Wang, X.; Zhou, H.; Zou, C.; Gao, M.; Zhang, Y.; Wu, Y. Study on the Synergy Between Silica Nanoparticles and Surfactants for Enhanced Oil Recovery During Spontaneous Imbibition. *J. Mol. Liq.* **2018**, *261*, 373–378. [[CrossRef](#)]
12. Soleimani, H.; Baig, M.K.; Yahya, N.; Khodapanah, L.; Sabet, M.; Demiral, B.M.; Burda, M. Synthesis of ZnO Nanoparticles for Oil–Water Interfacial Tension Reduction in Enhanced Oil Recovery. *Appl. Phys. A* **2018**, *124*, 128. [[CrossRef](#)]
13. Divandari, H.; Hemmati-Sarapardeh, A.; Schaffie, M.; Ranjbar, M. Integrating Synthesized Citric Acid-Coated Magnetite Nanoparticles with Magnetic Fields for Enhanced Oil Recovery: Experimental Study and Mechanistic Understanding. *J. Pet. Sci. Eng.* **2019**, *174*, 425–436. [[CrossRef](#)]
14. Seoud, O.A.E.; Keppeler, N.; Malek, N.I.; Galgano, P.D. Ionic Liquid-Based Surfactants: Recent Advances in Their Syntheses, Solution Properties, and Applications. *Polymers* **2021**, *13*, 1100. [[CrossRef](#)] [[PubMed](#)]
15. Ma, X.K.; Lee, N.H.; Oh, H.J.; Kim, J.W.; Rhee, C.K.; Park, K.S.; Kim, S.J. Surface Modification and Characterization of Highly Dispersed Silica Nanoparticles by a Cationic Surfactant. *Colloids Surf. A Physicochem. Eng. Asp.* **2010**, *358*, 172–176. [[CrossRef](#)]
16. Liu, L.; Gao, B.; Wu, L.; Sun, Y.; Zhou, Z. Effects of Surfactant Type and Concentration on Graphene Retention and Transport in Saturated Porous Media. *Chem. Eng. J.* **2015**, *262*, 1187–1191. [[CrossRef](#)]
17. Panahpoori, D.; Rezvani, H.; Parsaei, R.; Riazi, M. A Pore-Scale Study on Improving CTAB Foam Stability in the Heavy Crude Oil–Water System Using TiO₂ Nanoparticles. *J. Pet. Sci. Eng.* **2019**, *183*, 106411. [[CrossRef](#)]
18. Pereira, M.L.D.O.; Maia, K.C.; Silva, W.C.; Leite, A.C.; Francisco, A.D.D.S.; Vasconcelos, T.L.; Nascimento, R.S.; Grasseschi, D. Fe₃O₄ Nanoparticles as Surfactant Carriers for Enhanced Oil Recovery and Scale Prevention. *ACS Appl. Nano Mater.* **2020**, *3*, 5762–5772. [[CrossRef](#)]
19. Joshi, D.; Kumar, N.; Maurya, N.K.; Mandal, A. Experimental Investigation of Silica Nanoparticle Assisted Surfactant and Polymer Systems for Enhanced Oil Recovery. *J. Pet. Sci. Eng.* **2022**, *216*, 110791. [[CrossRef](#)]
20. Hethnawi, A.; Ashoorian, S.; Hashlamoun, K.; Contreras-Mateus, M.; Sagala, F.; Nassar, N.N. Influence of CTAB-Grafted Faujasite Nanoparticles on the Dynamic Interfacial Tension of Oil/Water Systems. *Energy Fuels* **2022**, *36*, 5666–5680. [[CrossRef](#)]
21. Pinazo, A.; Manresa, M.A.; Marques, A.M.; Bustelo, M.; Espuny, M.J.; Pérez, L. Amino Acid-Based Surfactants: New Antimicrobial Agents. *Adv. Colloid Interface Sci.* **2016**, *228*, 17–39. [[CrossRef](#)]
22. Atta, D.Y.; Negash, B.M.; Yekeen, N.; Habte, A.D. A State-Of-The-Art Review on the Application of Natural Surfactants in Enhanced Oil Recovery. *J. Mol. Liq.* **2021**, *321*, 114888. [[CrossRef](#)]
23. Nowrouzi, I.; Mohammadi, A.H.; Manshad, A.K. Preliminary Evaluation of a Natural Surfactant Extracted from Myrtus Communis Plant for Enhancing Oil Recovery From Carbonate Oil Reservoirs. *J. Pet. Explor. Prod. Technol.* **2022**, *12*, 783–792. [[CrossRef](#)]
24. Khayati, H.; Moslemzadeh, A.; Shahbazi, K.; Moraveji, M.K.; Riazi, S.H. An Experimental Investigation on the Use of Saponin as a Non-ionic Surfactant for Chemically Enhanced Oil Recovery (EOR) in Sandstone and Carbonate Oil Reservoirs: IFT, Wettability Alteration, and Oil Recovery. *Chem. Eng. Res. Des.* **2020**, *160*, 417–425. [[CrossRef](#)]
25. Emadi, S.; Shadizadeh, S.R.; Manshad, A.K.; Rahimi, A.M.; Nowrouzi, I.; Mohammadi, A.H. Effect of Using Zyziphus Spina Christi or Cedr Extract (Ce) As a Natural Surfactant on Oil Mobility Control by Foam Flooding. *J. Mol. Liq.* **2019**, *293*, 111573. [[CrossRef](#)]
26. Pal, N.; Kumar, N.; Verma, A.; Ojha, K.; Mandal, A. Performance Evaluation of Novel Sunflower Oil-Based Gemini Surfactant (s) With Different Spacer Lengths: Application in Enhanced Oil Recovery. *Energy Fuels* **2018**, *32*, 11344–11361. [[CrossRef](#)]
27. Traiwiriyawong, P.; Kungsanant, S. Potential of Palm Kernel Alkanolamide Surfactant for Enhancing Oil Recovery from Sandstone Reservoir Rocks. *Environ. Nat. Resour. J.* **2020**, *18*, 333–344. [[CrossRef](#)]
28. Wang, J.; Yang, L.; Xie, J.; Wang, Y.; Wang, T.J. Surface Amination of Silica Nanoparticles Using Tris (Hydroxymethyl) Aminomethane. *Ind. Eng. Chem. Res.* **2020**, *59*, 21383–21392. [[CrossRef](#)]
29. Habibi, S.; Jafari, A.; Fakhroueian, Z. Application of Novel Functionalized Al₂O₃/Silica by Organosiloxane and Amine Reagents for Enhanced Oil Recovery. *Appl. Nanosci.* **2020**, *10*, 2085–2100. [[CrossRef](#)]
30. Wang, J.; Xing, S.; Xie, J.; Zhao, S.; Gan, Y.; Yang, L.; Wang, T.J. Amination of Silica Nanoparticles Using Aminobutanol to Increase Surface Reactivity. *Colloids Surf. A Physicochem. Eng. Asp.* **2022**, *653*, 129958. [[CrossRef](#)]
31. Mattax, C.C.; Kyte, J.R. Imbibition Oil Recovery from Fractured, Water-Drive Reservoir. *Soc. Pet. Eng. J.* **1962**, *2*, 177–184. [[CrossRef](#)]
32. Ma, S.M.; Zhang, X.; Morrow, N.R.; Zhou, X. Characterization of Wettability from Spontaneous Imbibition Measurements. *J. Can. Pet. Technol.* **1999**, *38*, 94–97. [[CrossRef](#)]
33. Aronofsky, J.S.; Masse, L.; Natanson, S.G. A Model for the Mechanism of Oil Recovery from the Porous Matrix Due to Water Invasion in Fractured Reservoirs. *Trans. AIME* **1958**, *213*, 17–19. [[CrossRef](#)]

34. Navaie, F.; Esmailnezhad, E.; Choi, H.J. Xanthan Gum-Added Natural Surfactant Solution of Chuback: A Green and Clean Technique for Enhanced Oil Recovery. *J. Mol. Liq.* **2022**, *354*, 118909. [[CrossRef](#)]
35. Azarshin, S.; Moghadasi, J.; Aboosadi, Z.A. Surface Functionalization of Silica Nanoparticles to Improve the Performance of Water Flooding in Oil-Wet Reservoirs. *Energy Explor. Exploit.* **2017**, *35*, 685–697. [[CrossRef](#)]
36. Aryanti, N.; Nafiunisa, A.; Kusworo, T.D.; Wardhani, D.H. Dye Solubilization Ability of Plant-Derived Surfactant from Sapindus Rarak DC. Extracted With the Assistance of Ultrasonic Waves. *Environ. Technol. Innov.* **2021**, *22*, 101450. [[CrossRef](#)]
37. Garmroudi, A.; Kheirollahi, M.; Mousavi, S.A.; Fattahi, M.; Mahvelati, E.H. Effects of Graphene Oxide/TiO₂ Nanocomposite, Graphene Oxide Nanosheets, and Cedar Extraction Solution on IFT Reduction and Ultimate Oil Recovery from a Carbonate Rock. *Petroleum* **2020**, *8*. [[CrossRef](#)]
38. Nowrouzi, I.; Mohammadi, A.H.; Manshad, A.K. Water-Oil Interfacial Tension (IFT) Reduction and Wettability Alteration in Surfactant Flooding Process Using Extracted Saponin from Anabasis Setifera Plant. *J. Pet. Sci. Eng.* **2020**, *189*, 106901. [[CrossRef](#)]
39. Khademolhosseini, R.; Jafari, A.; Mousavi, S.M.; Manteghian, M.; Fakhroueian, Z. Synthesis of Silica Nanoparticles with Different Morphologies and Their Effects on Enhanced Oil Recovery. *Appl. Nanosci.* **2020**, *10*, 1105–1114. [[CrossRef](#)]
40. Meng, X.; Yang, D. Critical Review of Stabilized Nanoparticle Transport in Porous Media. *J. Energy Resour. Technol.* **2019**, *141*, 070801. [[CrossRef](#)]
41. Kazemzadeh, Y.; Dehdari, B.; Etemadan, Z.; Riazi, M.; Sharifi, M. Experimental Investigation into Fe₃O₄/SiO₂ Nanoparticle Performance and Comparison with Other Nanofluids in Enhanced Oil Recovery. *Pet. Sci.* **2019**, *16*, 578–590. [[CrossRef](#)]
42. Agista, M.N.; Guo, K.; Yu, Z. A State-Of-The-Art Review of Nanoparticles Application in Petroleum with a Focus on Enhanced Oil Recovery. *Appl. Sci.* **2018**, *8*, 871. [[CrossRef](#)]
43. Olayiwola, S.O.; Dejam, M. Comprehensive Experimental Study on the Effect of Silica Nanoparticles on the Oil Recovery During Alternating Injection with Low Salinity Water and Surfactant into Carbonate Reservoirs. *J. Mol. Liq.* **2021**, *325*, 115178. [[CrossRef](#)]
44. Bagherpour, S.; Rashidi, A.; Mousavi, S.H.; Izadi, N.; Hamidpour, E. Experimental Investigation of Carboxylate-Alumoxane Nanoparticles for the Enhanced Oil Recovery Performance. *Colloids Surf. A Physicochem. Eng. Asp.* **2019**, *563*, 37–49. [[CrossRef](#)]
45. Norouzpour, M.; Nabipour, M.; Azdarpour, A.; Akhondzadeh, H.; Santos, R.M.; Keshavarz, A. Experimental Investigation of the Effect of a Quinoa-Derived Saponin-Based Green Natural Surfactant on Enhanced Oil Recovery. *Fuel* **2022**, *318*, 123652. [[CrossRef](#)]
46. Tufenkji, N.; Elimelech, M. Deviation from the Classical Colloid Filtration Theory in the Presence of Repulsive DLVO Interactions. *Langmuir* **2004**, *20*, 10818–10828. [[CrossRef](#)]
47. Bayat, A.E.; Junin, R.; Samsuri, A.; Piroozian, A.; Hokmabadi, M. Impact of Metal Oxide Nanoparticles on Enhanced Oil Recovery from Limestone Media at Several Temperatures. *Energy Fuels* **2014**, *28*, 6255–6266. [[CrossRef](#)]
48. Meng, Q.; Liu, H.; Wang, J. A Critical Review on Fundamental Mechanisms of Spontaneous Imbibition and the Impact of Boundary Condition, Fluid Viscosity, and Wettability. *Adv. Geoenery Res.* **2017**, *1*, 1–17. [[CrossRef](#)]
49. Chen, P.; Mohanty, K.K. Surfactant-Enhanced Oil Recovery from Fractured Oil-Wet Carbonates: Effects of Low IFT and Wettability Alteration. In Proceedings of the SPE International Symposium on Oilfield Chemistry, The Woodlands, TX, USA, 13–15 April 2015.
50. Ghasemian, J.; Riahi, S. Effects of Salinity, and Ionic Composition of Smart Water on Mineral Scaling in Carbonate Reservoirs during Water Flooding. *Pet. Explor. Dev.* **2021**, *48*, 421–429. [[CrossRef](#)]
51. Sarafzadeh, P.; Hezave, A.Z.; Ravanbakhsh, M.; Niazi, A.; Ayatollahi, S. Enterobacter Cloacae as Biosurfactant Producing Bacterium: Differentiating Its Effects on Interfacial Tension and Wettability Alteration Mechanisms for Oil Recovery During MEOR Process. *Colloids Surf. B Biointerfaces* **2013**, *105*, 223–229. [[CrossRef](#)]
52. Jahanbin, K. Structural Characterization of a New Water-Soluble Polysaccharide Isolated from Acanthophyllum Acerosum Roots and Its Antioxidant Activity. *Int. J. Biol. Macromol.* **2018**, *107*, 1227–1234. [[CrossRef](#)]
53. Nowrouzi, I.; Mohammadi, A.H.; Manshad, A.K. Characterization and Likelihood Application of Extracted Mucilage from Hollyhocks Plant as a Natural Polymer in the Enhanced Oil Recovery Process by Alkali-Surfactant-Polymer (ASP) Slug Injection into Sandstone Oil Reservoirs. *J. Mol. Liq.* **2020**, *320*, 114445. [[CrossRef](#)]
54. Hong, T.; Yin, J.Y.; Nie, S.P.; Xie, M.Y. Applications of Infrared Spectroscopy in Polysaccharide Structural Analysis: Progress, Challenge, and Perspective. *Food Chem. X* **2021**, *12*, 100168. [[CrossRef](#)] [[PubMed](#)]
55. Polat, S.; Sayan, P. Assessment of the Thermal Pyrolysis Characteristics and Kinetic Parameters of Spent Coffee Waste: A TGA-MS Study. *Energy Sources A Recovery Util. Environ. Eff.* **2020**, *42*, 1–14. [[CrossRef](#)]
56. Liu, Y.; Li, R.; Yu, J.; Ni, F.; Sheng, Y.; Scircle, A.; Cizdziel, J.V.; Zhou, Y. Separation, and Identification of Microplastics in Marine Organisms by TGA-FTIR-GC/MS: A Case Study of Mussels from Coastal China. *Environ. Pollut.* **2021**, *272*, 115946. [[CrossRef](#)]
57. Dashtaki, S.R.M.; Ali, J.A.; Manshad, A.K.; Nowrouzi, I.; Mohammadi, A.H.; Keshavarz, A. Experimental investigation of the effect of Vitagnus plant extract on enhanced oil recovery process using interfacial tension (IFT) reduction and wettability alteration mechanisms. *J. Pet. Explor. Prod. Technol.* **2020**, *10*, 2895–2905. [[CrossRef](#)]
58. Kaimal, R.; Vinoth, V.; Salunke, A.S.; Valdés, H.; Mangalaraja, R.V.; Aljafari, B.; Anandan, S. Highly Sensitive and Selective Detection of Glutathione Using Ultrasonic Aided Synthesis of Graphene Quantum Dots Embedded Over Amine-Functionalized Silica Nanoparticles. *Ultrason. Sonochem.* **2022**, *82*, 105868. [[CrossRef](#)]
59. Zhou, Y.; Wu, X.; Zhong, X.; Sun, W.; Pu, H.; Zhao, J.X. Surfactant-Augmented Functional Silica Nanoparticle-Based Nanofluid for Enhanced Oil Recovery at High Temperature and Salinity. *ACS Appl. Mater. Interfaces* **2019**, *11*, 45763–45775. [[CrossRef](#)]
60. Petreanu, I.; Niculescu, V.C.; Enache, S.; Iacob, C.; Teodorescu, M. Structural Characterization of Silica and Amino-Silica Nanoparticles by Fourier Transform Infrared (FTIR) and Raman Spectroscopy. *Anal. Lett.* **2022**, *55*, 1–14. [[CrossRef](#)]

61. Reddy, B.M.; Saikia, P.; Bharali, P.; Katta, L.; Thrimurthulu, G. Highly Dispersed Ceria, and Ceria-Zirconia Nanocomposites Over Silica Surfaces for Catalytic Applications. *Catal. Today* **2009**, *141*, 109–114. [[CrossRef](#)]
62. Nowrouzi, I.; Manshad, A.K.; Mohammadi, A.H. Effects of Concentration and Size of TiO₂ Nano-Particles on the Performance of Smart Water in Wettability Alteration and Oil Production Under Spontaneous Imbibition. *J. Pet. Sci. Eng.* **2019**, *183*, 106357. [[CrossRef](#)]
63. Khosravi, R.; Chahardowli, M.; Keykhosravi, A.; Simjoo, M. A Model for Interpretation of Nanoparticle-Assisted Oil Recovery: Numerical Study of Nanoparticle-Enhanced Spontaneous Imbibition Experiments. *Fuel* **2021**, *292*, 120174. [[CrossRef](#)]
64. Rostami, P.; Sharifi, M.; Aminshahidy, B.; Fahimpour, J. Enhanced Oil Recovery Using Silica Nanoparticles in the Presence of Salts for Wettability Alteration. *J. Dispers. Sci. Technol.* **2019**, *41*, 402–413. [[CrossRef](#)]
65. Khoramian, R.; Kharrat, R.; Golshokoh, S. The Development of Novel Nanofluid for Enhanced Oil Recovery Application. *Fuel* **2021**, *311*, 122558. [[CrossRef](#)]
66. Khoramian, R.; Ramazani, S.A.A.; Hekmatzadeh, M.; Kharrat, R.; Asadian, E. Graphene Oxide Nanosheets for Oil Recovery. *ACS Appl. Nano Mater.* **2019**, *2*, 5730–5742. [[CrossRef](#)]
67. Standnes, D.C. Scaling Group for Spontaneous Imbibition Including Gravity. *Energy Fuels* **2010**, *24*, 2980–2984. [[CrossRef](#)]
68. Keykhosravi, A.; Simjoo, M. Enhancement of Capillary Imbibition by Gamma-Alumina Nanoparticles in Carbonate Rocks: Underlying Mechanisms and Scaling Analysis. *J. Pet. Sci. Eng.* **2020**, *187*, 106802. [[CrossRef](#)]
69. Xu, D.; Bai, B.; Wu, H.; Hou, J.; Meng, Z.; Sun, R.; Li, Z.; Lu, Y.; Kang, W. Mechanisms of Imbibition Enhanced Oil Recovery in Low Permeability Reservoirs: Effect of IFT Reduction and Wettability Alteration. *Fuel* **2019**, *244*, 110–119. [[CrossRef](#)]
70. Morrow, N.R.; Mason, G. Recovery of Oil by Spontaneous Imbibition. *Curr. Opin. Colloid Interface Sci.* **2001**, *6*, 321–337. [[CrossRef](#)]
71. Li, K.; Horne, R.N. Generalized Scaling Approach for Spontaneous Imbibition: An Analytical Model. *SPE Reserv. Eval. Eng.* **2006**, *9*, 251–258. [[CrossRef](#)]
72. Nazari Moghaddam, R.; Bahramian, A.; Fakhroueian, Z.; Karimi, A.; Arya, S. Comparative Study of Using Nanoparticles for Enhanced Oil Recovery: Wettability Alteration of Carbonate Rocks. *Energy Fuels* **2015**, *29*, 2111–2119. [[CrossRef](#)]
73. Gbadamosi, A.O.; Junin, R.; Manan, M.A.; Agi, A.; Oseh, J.O.; Usman, J. Effect of Aluminum Oxide Nanoparticles on Oilfield Polyacrylamide: Rheology, Interfacial Tension, Wettability, and Oil Displacement Studies. *J. Mol. Liq.* **2019**, *296*, 111863. [[CrossRef](#)]
74. Rezvani, H.; Tabaei, M.; Riazi, M. Pore-Scale Investigation of Al₂O₃ Nanoparticles for Improving Smart Water Injection: Effect of Ion Type, Ion and Nanoparticle Concentration, and Temperature. *Mater. Res. Express* **2019**, *6*, 085505. [[CrossRef](#)]